Analysis of Vis/NIR Spectral Variations of Wholesome, Septicemia, and Cadaver Chicken Samples

K. Chao, Y. R. Chen, D. E. Chan

Abstract. *The Instrumentation and Sensing Laboratory, ARS, USDA, has developed a Vis/NIR spectroscopic system for on–line poultry carcass inspection. This system was proven to be effective in distinguishing between wholesome and unwholesome carcasses. To better understand how the carcasses can be differentiated, a further in–depth study of Vis/NIR spectra of poultry samples was conducted. Results showed that Vis/NIR spectroscopy can be used to differentiate poultry samples more finely than merely between a wholesome category and a broadly inclusive unwholesome category. Using principal component analysis (PCA) and discriminant analysis, wholesome, septicemia, and cadaver chicken samples were differentiated from each other with high accuracy. The best Vis/NIR classification model, using nine principal components (PCs) and a linear discriminant function, correctly classified 100%, 90.0%, and 92.5% of the whole (skin and meat) samples for wholesome, septicemia, and cadaver categories, respectively. For skin only samples, similar models using nine PCs resulted in lower accuracies. Examination of the PCA loadings for the whole samples suggested that the better discrimination of whole samples was dependent on spectral variation related to different forms of myoglobin present in the chicken meat, i.e. deoxymyoglobin, metmyoglobin, and oxymyoglobin. In particular, key wavelengths were identified at 540 and 585 nm, which have been identified as oxymyoglobin bands, for PCs 1 and 2; 485 nm, metmyoglobin, for PC 3; and 440 nm, deoxymyoglobin, for PC 8.*

Keywords. *Food safety, Poultry inspection, Visible/near–infrared spectroscopy, Myoglobin.*

Currently, each chicken intended for sale to U.S. consumers is required by law to be inspected post–mortem by a United States Department of Agriculture/Food Safety and Inspection Service (USDA/FSIS) inspector for its wholesomeness (USDA, 1984). These inspectors visually and manually inspect poultry carcasses and viscera on–line at processing plants. They are trained to recognize infectious condition and avian diseases, dressing defects, fecal and digestive content contamination, and conditions that are related to many other consumer protection concerns.

FSIS has just completed a 3–year transformation of its traditional inspection system to a Hazard–Analysis–and–Critical–Control–Point (HACCP) inspection system. Under this system, FSIS inspectors still do a bird–by–bird organoleptic examination, but FSIS personnel also monitor a producer–run HACCP plan, which is developed by each plant and approved by FSIS. The HACCP system, together with the demands of increased production, has increased the workload of FSIS plant personnel, while fixed budgets have restricted the ability of FSIS to meet these demands.

Under HACCP, FSIS has now started testing a change in the division of responsibilities between government and producers in a few plants, called the HACCP–based Inspections Models Project (HIMP). Under HIMP, the processing plants are responsible for delivering poultry carcasses free of infectious condition and fecal contamination (two food safety categories, FS1 and FS2). They are also responsible for meeting requirements for five other consumer protection (OCP) issues determined by FSIS. The producers assume the responsibility for the bird–by–bird inspection, and FSIS performs oversight and verification duties to ensure that FSIS standards are met. Under these models, the heavy inspection workload shifts to the producers. FSIS, however, retains the authority to take whatever steps are necessary to ensure that the zero–tolerance standards for FS1 and FS2 are met.

Under either HACCP or HIMP, increasing consumer demand and line speeds will continue to increase the need for and pressure on inspectors. Thus, to address food safety concerns and meet growing consumer demand, there is an urgent need to develop automated inspection systems that can operate on–line in real–time [at least 140 birds–per–minute (bpm)] in the slaughter plant environment. These systems should be able to accurately detect and identify carcasses with infectious condition, particularly septicemia/toxemia, and fecal contamination. They should also detect avian diseases, particularly airsacculitis, ascites, cadaver, and inflammatory process (IP). In developing such systems, usually involving spectral and/or imaging techniques, it is essential to first identify key wavelengths, then develop algorithms based on those wavelengths, and finally implement them for on–line applications. For example, studies

Aticle was submitted for review in January 2003; approved for publication by Food & Process Engineering Institute Division of ASAE in May 2003.

Mention of trade names or commercial products is solely for the purpose of providing specific information and does not imply endorsement of recommendation by the USDA.

The authors are **Kuanglin Chao,** Research Scientist, **Yud–Ren Chen, ASAE Member Engineer,** Research Leader, and **Diane E.Chan,** Agricultural Engineer, USDA/ARS/ISL, Beltsville, Maryland. **Corresponding author:** Kuanglin Chao, USDA/ARS/ISL, Building 303, BARC–East, 10300 Baltimore Avenue, Beltsville, MD 20705–2350; phone: 301–504–8450; fax: 301–504–9466; e–mail: chaok@ba.ars.usda.gov.

(Windham et al., 2001; Lawrence et al., 2001; Park et al., 2002) to detect fecal contamination on poultry carcasses have used a visible/near–infrared (Vis/NIR) monochromator to identify wavelengths associated with fecal absorption bands, and then, using hyperspectral imaging, evaluated those wavelengths and developed image–processing algorithms. For poultry carcass inspection, wavelengths associated with infection conditions have been identified using hyperspectral imaging, and then implemented in multispectral imaging and dual–camera systems (Chao et al., 2002a, 2002b).

Vis/NIR spectroscopy is a method that is appropriate for both the development and implementation of a poultry inspection system. Vis/NIR spectrometry can be used to measure both physical and chemical properties of agricultural products, by–products, and food. Because unwholesome carcasses often have a variety of visible skin and tissue changes, these carcasses can be detected with a Vis/NIR spectroscopic technique. Recent research on food safety inspection of chicken carcasses using Vis/NIR spectroscopy has included: the selection of optimal wavelengths for correlating spectral reflectance and interactance with the condition of poultry carcasses (Chen and Massie, 1993); offline carcass classification (Chen et al., 1998a); and development of a transportable photodiode array spectrophotometer for on–line inspection of poultry carcasses (Chen et al., 2000). The on–line transportable Vis/NIR system was proven to be effective in distinguishing between wholesome and unwholesome carcasses on a processing line at 70 bpm. Classification models, using principal component analysis as a data pretreatment for input into neural networks, were able to classify the carcasses with a success rate of 95%. To better understand how the carcasses can be differentiated, a further in–depth study of Vis/NIR spectra of poultry was conducted.

The objectives of this study were: (1) to determine whether Vis/NIR could differentiate between specific unwholesome poultry categories based upon the absorbance spectra of skin samples as well as skin–and–meat samples, and (2) to understand the chemical basis for the Vis/NIR classification models.

Materials and Methods

Chicken Carcasses

Chicken carcasses were identified as belonging to one of three inspection categories: wholesome, septicemia, and cadaver (40 in each category). Septicemia is a systemic disease caused by pathogenic microorganisms in the blood. Cadaver is caused by improper slaughter cuts or inadequate bleeding time.

These chicken carcasses were identified and collected by USDA FSIS veterinarians from Allen Family Foods (Cordova, Md.). Chicken carcasses were marked according to the condemnation conditions and placed in plastic bags to minimize dehydration. Then the bags were placed in coolers, covered with ice, and transported to the Instrumentation and Sensing Laboratory (ISL) located in Beltsville, Maryland, within 2 h for the experiments.

Visible/Near–Infrared Reflection Measurement Equipment

Spectral reflectance data of samples cut from poultry carcasses were collected using a photodiode array spectrophotometer. The spectrophotometer system (fig. 1) consisted of a tungsten halogen light source and power supply, a bifurcated fiber–optic probe (diameter 25.4 mm) assembly, a spectrograph, a photodiode array detector, and a personal computer with a photodiode array computer interface card installed. The spectrograph (Oriel model 77400) had a focal length of 120 mm, a grating ruling of 400 lines/mm and a reciprocal dispersion of 20.9 nm/mm. At the exit of the spectrograph was a 1024–silicon photodiode detector (Oriel model 78220) element head. With this setup, the average spectral sampling interval was slightly less than 0.5 nm. The temperature of the photodiode array was thermoelectrically regulated to 20 ± 0.1°C to reduce dark current drift and ensure signal stability. The photodiode array detector head was connected via a cable to a personal computer interface controller card (Oriel model CC100). This interface card provided a 16–bit analog–to–digital converter that converts the analog signal from each diode to a digitized number and transfers the data to the personal computer.

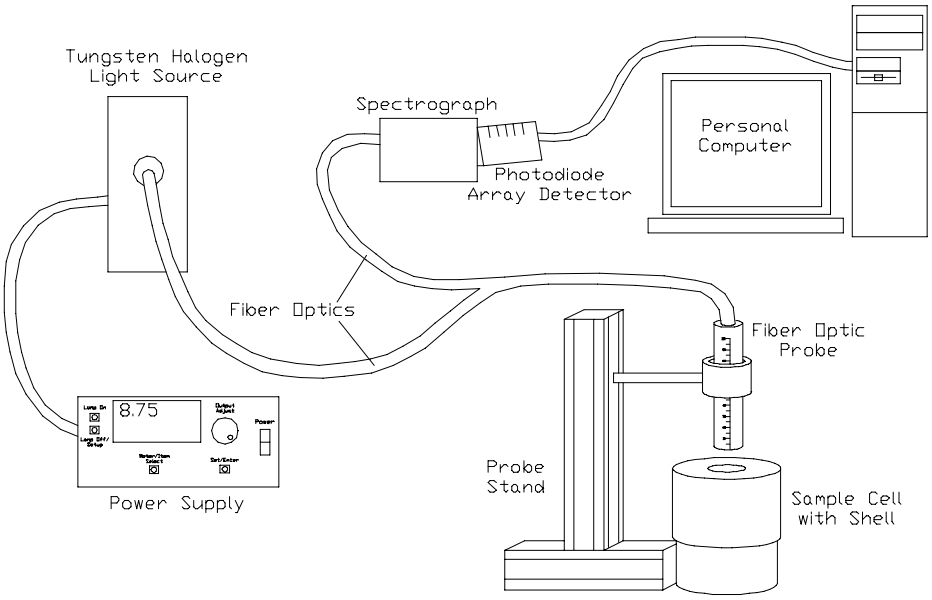

Figure 1. Schematic of spectrophotometer system.

Light from a 100–W quartz tungsten halogen light bulb was focused on the light source circular end of a 1.2–m bifurcated fiber–optic bundle (Schott–Fostec, Auburn, N.Y.) with the use of a condensing/imaging lens assembly (*f*/1.8, 33–mm aperture, UV–grade fused silica). A radiometric constant–current dc power supply (Oriel model 68831) was used to keep the light intensity constant and minimize color temperature shift as a result of power line fluctuations. This light energy traveled through the fiber–optic cable and exited by means of a concentric ring of optical fibers (diameter 15.8 mm, thickness 1.1 mm), to be focused on the chicken sample surface. After interacting with the chicken sample, the light energy was then collected through a 7.5–mm diameter aperture in the center of the concentric optical probe. The collected energy was transmitted back through the bifurcated fiber–optic cable to a 4–mm high × 50–μm wide exit rectangle (slit) on the spectrograph ferrule. The fixed entrance slit of the spectrograph was 3–mm high × 25–μm wide.

Measurement Procedure

The sample holder was a cylindrical white Teflon cell with an interior chamber measuring 5 cm in height and 5 cm in diameter. The walls and base of the cylinder were 1.5 cm thick. Each sample was placed flat in the bottom of the cylinder. The probe was mounted in the cylinder so that the distance from the probe to the sample was about 2 cm. Before measuring the reflectance of each sample, background and white reference measurements were taken. A dark reference (background measurement) was taken to compensate for the zero energy signal by placing the probe 2 cm from the bottom of the empty sample cell with the light source turned off. A white reference measurement was taken to establish a spectrally flat repeatable high–energy reference by placing the fiber–optic probe 2 cm from the bottom of the empty sample cell with the light source turned on. Spectra were recorded as percent according to the formula

$$\% \text{ Reflectance} = 100 \times (\text{sample reflectance} - \text{dark reference}) / (\text{white reference} - \text{dark reference}) \quad (1)$$

For each carcass, the right breast was removed with the skin intact. Then a 49–mm diameter cylinder was cut out. The skin, approximately 4 mm thick, was removed and set aside while the meat was sliced to a thickness of 15 mm. To take a reflectance measurement of a skin and meat sample (hereafter called a "whole" sample), the cylinder of chicken meat with skin overlaid was placed in the sample cell and the fiber–optic probe was positioned 2 cm above the surface of the sample. The meat was then removed from the cell, leaving only the skin. The probe was repositioned 2 cm above the surface of the skin and reflectance was measured. This procedure resulted in two reflectance measurements for each sample, one for the whole sample (skin and meat) and one for the skin sample. With 40 samples in each of the three categories (wholesome, septicemia, cadaver), a total of 240 spectra were measured, two spectra (whole and skin) for each of the 120 samples.

The spectrophotometer measured the spectral reflectance of each sample in the wavelength range of 411.33 to 923.41 nm. Each spectrum was composed of 1024 data points measured at intervals slightly less than 0.5 nm. In an effort to improve the signal–to–noise ratio, each spectrum was the sum/accumulation of 244 scans of the diode array, where each scan was the result of a 0.0328–s photodiode array exposure. This setting resulted in an 8.0032–s total scan. Absorbance spectra were obtained by transforming each spectrum into log (1/Reflectance) for data analysis.

Multivariate Data Analysis and Modeling

Principal component analysis (PCA) (PRINCOMP, Mathworks Inc., Natick, Mass.) used for data analysis is a projection method for the extraction of systematic variations in a dataset. Two PCA spectra datasets were created, one for whole samples and one for skin samples, each containing 120 spectra. Each spectra dataset was transformed onto principal components (PCs), a new coordinate system of fewer dimensions than the original visible/NIR dataset (of wavelength coordinates). The directions of the new principal component coordinate axes describe the largest variations. The coefficients of the sample spectra in the new system, i.e., their coordinates related to the PCs, are called scores.

Scores for the first 15 PCs were used in a SAS 6.12 (SAS Institute Inc., Cary, N.C.) procedure (PROC STEPDISC) for identifying, by stepwise search, the components that were most important in separating the sample categories. STEPDISC uses forward selection and backward elimination to select a subset of components for classifying each sample spectrum into individual categories. The stepwise search procedure was followed by the DISCRIM procedure to evaluate selected components, by cross–validation, the optimal number of components to use in a discriminant function for sample classification. With the assumption that independent variables (PCs) were multivariate normally distributed in each sample category (wholesome, septicemia, and cadaver), and with the pooling of the covariance matrix across the sample category, a linear discriminant function was used for the DISCRIM procedure. Alternatively, a quadratic discriminant function also was used, based on no pooling of the covariance matrices.

Results and Discussion

Figure 2 shows the average absorbance [log (1/reflectance)] spectra of whole samples for the three different chicken categories. In general, the septicemia and cadaver sample spectra had higher absorbance than wholesome sample spectra. Differences in absorbance value between the wholesome and unwholesome chicken samples decreased as wavelength increased. In particular, differences in absorbance value between wholesome and unwholesome chickens were larger in the visible region (400 to 700 nm) than in the NIR region. Myoglobin, which comprises 50% to 80% of meat pigment mass, is primarily responsible for the absorbance features in this region (Kinsman et al., 1994; Swatland, 1989). Liu et al. (2000) reported that there are at least seven absorption bands at 415, 424, 445, 475, 520, 560, and 585 nm associated with the changes due to the oxidation and denaturation of myoglobin during treatment processes such as cooking and cold storage. The most distinctive difference in absorption bands among the three types of whole samples occurred at 540 and 575 nm. The bands at 540 and 575 nm, which are attributed to oxymyoglobin, and 485 nm, metmyoglobin, are absorption areas that form a major

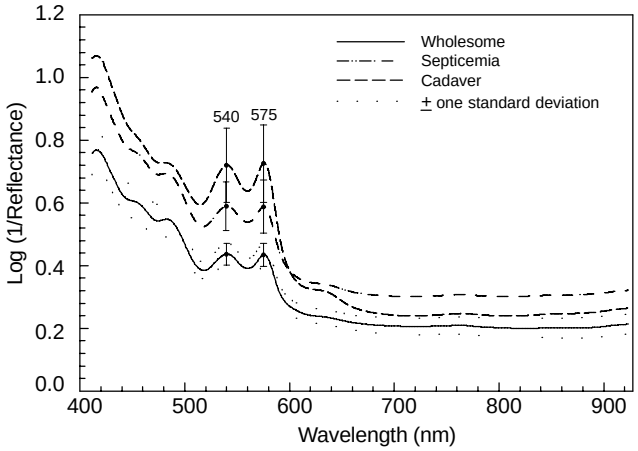

Figure 2. Average absorbance (log 1/Reflectance) spectra of whole samples for wholesome, septicemia, and cadaver category, with ± one standard deviation envelope (dotted line).

base for spectral differentiation of wholesome chicken from unwholesome chicken (Liu and Chen, 2001).

Figure 3 depicts the average absorbance [log (1/reflectance)] spectra of skin samples for each of the three different chicken categories. The average spectrum for each of the three categories, along with the two–sided standard deviation envelope for the wholesome category, indicated that spectral variation within a single category was often as large as that between categories, especially in the near–infrared region. The skin samples had lower absorbance (higher reflectance) than the whole samples. The two distinct absorption bands at 540 and 575 nm were also observed in the spectra of the skin samples. Despite this similarity, differences between the skin and whole sample spectra in this study show that the incident light does penetrate through beyond the skin to reach the underlying tissue where infectious disease symptoms occur.

Tables 1 and 2 show the results of using the absorbance values at 540 and 575 nm in two–wavelength classification models (with one–sample–out cross validation) for whole samples and skin samples, respectively. The model using the linear discriminant function performed better than the model using the quadratic discriminant function, and achieved better separation for whole samples than for skin samples. For whole samples, 100%, 82.5%, and 82.5% of wholesome,

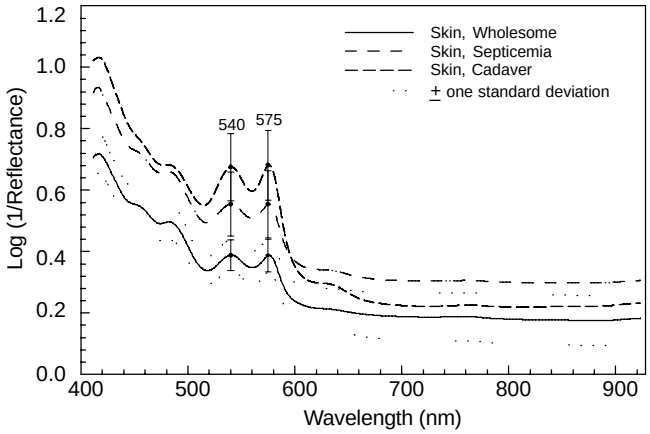

Figure 3. Average absorbance (log 1/Reflectance) spectra of skin samples for wholesome, septicemia, and cadaver category, with ± one standard deviation envelope (dotted line).

Table 1. Cross validation of whole samples, using two–wavelength model with linear or quadratic discriminant function.

Actual Category	Discriminant Functions	Assigned Category		
		Wholesome	Septicemia	Cadaver
Wholesome	linear	40 (100%)	0	0
	quadratic	37 (92.5%)	3	0
Septicemia	linear	2	33 (82.5%)	5
	quadratic	3	30 (75.0%)	7
Cadaver	linear	2	5	33 (82.5%)
	quadratic	2	6	32 (80.0%)

septicemia, and cadaver samples, respectively, were correctly identified. The skin samples were less accurately classified, with only 90.0% of wholesome samples, 62.5% of septicemia samples, and 75.0% of cadaver samples correctly identified.

Two PCA spectra datasets were generated, one for whole samples and one for skin samples. The first 15 components accounted for 99.98% and 99.99% of the total spectral variation for the dataset of whole samples and skin samples, respectively. Upon reduction of the spectral data by PCA, a stepwise search of the most important factors, in which up to 10 PCs were permitted, resulted in the selection of PC 1 as most useful for both the whole samples and skin samples (tables 3 and 4, respectively). With the first PC alone, the overall classification rate was nearly 70%, regardless of sample type or discriminant function (i.e., linear, quadratic). Adding PC 2 resulted in a large incremental increase in classification accuracy rate, with average increases of 15% and 8% in classification rate for whole samples and skin samples, respectively. With the inclusion of PC 3, the classification rates reached averages of 85% (84.4% linear and 87.2% quadratic) for whole samples and 81% (80.0% linear and 81.7% quadratic) for skin samples.

Interestingly, the fourth most important factor (PC 8 for whole samples, PC 15 for skin samples) did not coincide with that factor associated with the next greatest spectral variation. To further investigate this observation, the loadings associated with PCs 1, 2, 3, and 8 for whole samples are plotted in figure 4. The loading weights (being regression coefficients at specific wavelengths for a PC) show the relative contribution of those wavelengths to the amount of spectral variance for which that PC accounts. Thus a large positive or large negative weight indicates a significant contribution for the corresponding wavelength.

The shape of the plot for the first PC showed resemblance to an absorption spectrum, as do the shapes of PCs 2, 3, and 8. The loading weights for these PCs appear to reflect the presence of various forms of myoglobin. Liu and Chen (2000) determined several band assignments in chicken meat spectra for myoglobin and its derivatives, including deoxymyoglobin at 440 nm, metmyoglobin at 485 nm,

Table 2. Cross validation of skin samples, using two–wavelength model with linear or quadratic discriminant function.

Actual Category	Discriminant Functions	Assigned Category		
		Wholesome	Septicemia	Cadaver
Wholesome	linear	36 (90–.0%)	4	0
	quadratic	36 (90–.0%)	4	0
Septicemia	linear	5	25 (62.5%)	10
	quadratic	2	28 (70.0%)	10
Cadaver	linear	3	7	30 (75.0%)
	quadratic	3	9	28 (70.0%)

Table 3. Average percentage of correctly classified whole samples by cross validation. [a]

No. of Principal Components	Principal Components Selected	Average Percentage of Correctly Classified Samples	
		Linear Discriminant	Quadratic Discriminant
1	1	66.9	67.5
2	1,2	80.0	85.0
3	1,2,3	84.4	87.2
4	1,2,3,8	88.4	90.9
5	1,2,3,8,6	91.7	91.7
6	1,2,3,8,6,14	91.7	92.5
7	1,2,3,8,6,14,15	92.5	93.3
8	1,2,3,8,6,14,15,13	92.5	91.4
9	1,2,3,8,6,14,15,13,10	94.2	93.3
10	1,2,3,8,6,14,15,13,10,5	94.2	91.7

[a] Based on linear or quadratic discriminant function applied to principal component analysis scores.

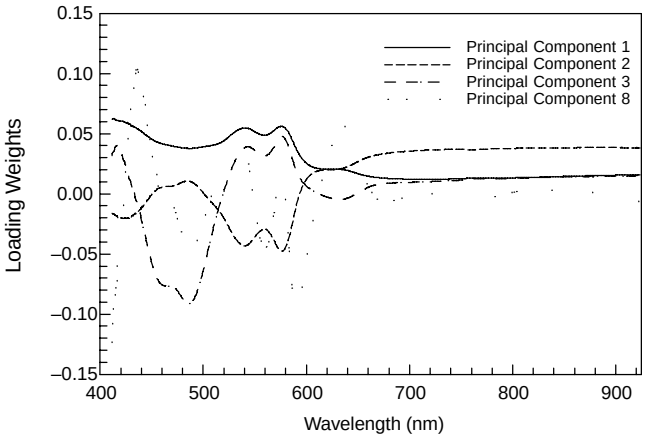

Figure 4. Loading weights of PCs 1, 2, 3, 8, determined from principal component analysis on whole samples.

oxymyoglobin at 540 and 585 nm. The PC loading weights suggest major contributions of oxymyoglobin (540 and 580 nm) to PCs 1 and 2, metmyoglobin (485 nm) and oxymyoglobin to PC 3, and all three myoglobin forms as well as sulfmyoglobin absorption (635 nm) to PC 8. Using four principal components (PCs 1, 2, 3, and 8), the overall classification accuracy rates were 88.4% (linear) and 90.9% (quadratic) for whole samples. The overall classification rates were 83.7% for linear and 85.9% for quadratic discriminant functions, respectively, for the skin samples when using PCs 1, 2, 3, and 15. For the skin samples, the increase in classification rate with each additional PC was smaller than that for whole samples, but was still significant.

As more principal components were added, the performance of the classification models generally improved. At nine PCs, the average percentage of correctly classified samples ranged between 87% and 94%, with little difference between the choice of discriminant function. With nine PCs, the actual numbers of correctly and incorrectly assigned samples by category are shown in tables 5 and 6 for whole samples and skin samples, respectively. For wholesome chicken, no more than 3 of the 40 samples from whole sample set, and 4 of the 40 samples from skin sample set, were misclassified. In each case, misclassification occurred as an assignment into the neighboring septicemic category. For unwholesome chicken samples (septicemia and cadaver), misclassification occurred more often than wholesome chicken. Misclassification of unwholesome chicken usually represented assignment into the neighboring septicemic or cadaver category, especially for the cadaver skin samples of which more than 6 of the 40 samples were misclassified as septicemia. Further improvements in classification rate made possible by using more than nine PCs were small in magnitude and significance. It is reasonable that the small number of PCs with major contributions from visible wavelength regions can adequately classify these three chicken categories, given the major color differences between wholesome, septicemia, and cadaver. However, considering that other categories of interest, such as airsacculitis and ascites, may not have such distinct visible differences, additional PCs with near–infrared wavelength contributions may be valuable in improving classification accuracy (Chen et al., 1998b).

Table 4. Average percentage of correctly classified skin samples by cross validation.[a]

No. of Principal Components	Principal Components Selected	Average Percentage of Correctly Classified Samples	
		Linear Discriminant	Quadratic Discriminant
1	1	71.7	68.4
2	1,2	78.4	79.2
3	1,2,3	80.0	81.7
4	1,2,3,15	83.7	85.9
5	1,2,3,15,8	84.2	86.7
6	1,2,3,15,8,4	87.5	82.5
7	1,2,3,15,8,4,14	86.7	82.5
8	1,2,3,15,8,4,14,6	87.5	88.4
9	1,2,3,15,8,4,14,6,5	87.7	90.0
10	1,2,3,15,8,4,14,6,5,11	88.4	86.7

[a] Based on linear or quadratic discriminant function applied to principal component analysis scores

Table 5. Cross validation of whole samples, using nine–factor principal component model with linear or quadratic discriminant function, for whole samples.

Actual Category	Discriminant Functions	Assigned category		
		Wholesome	Septicemia	Cadaver
Wholesome	linear	40 (100%)	0	0
	quadratic	37 (92.5%)	3	0
Wepticemia	linear	4	36 (90.0%)	0
	quadratic	1	36 (90.0%)	3
Cadaver	linear	1	2	37 (92.5%)
	quadratic	0	1	39 (97.5%)

Table 6. Cross validation of skin samples, using nine–factor principal component model with linear or quadratic discriminant function, for skin samples.

Actual Category	Discriminant Functions	Assigned Category		
		Wholesome	Septicemia	Cadaver
Wholesome	linear	37 (92.5%)	3	0
	quadratic	36 (90.0%)	4	0
Septicemia	linear	2	35 (87.5%)	3
	quadratic	1	38 (95.0%)	1
Cadaver	linear	1	7	32 (80.0%)
	quadratic	0	6	43 (85.0%)

CONCLUSIONS

The results of this study show that Vis/NIR spectroscopy can be used to differentiate poultry samples more finely than merely between a wholesome category and a broadly inclusive unwholesome category. Wholesome, septicemia, and cadaver chicken samples were differentiated from each other with high accuracy. The best Vis/NIR classification model, using 9 PCs and a linear discriminant function, correctly classified 100%, 90.0%, and 92.5% of the whole samples for wholesome, septicemia, and cadaver categories, respectively.

Although the classification models could differentiate wholesome, septicemia, and cadaver skin samples, the successful classification rates of skin samples were lower than those of whole samples, for both two–wavelength models and PCA models. Examination of the PCA loadings for the whole samples suggested that the better discrimination of whole samples was dependent on spectral variation related to different forms of myoglobin present in the chicken meat, i.e. deoxymyoglobin, metmyoglobin, oxymyoglobin, and sulfmyoglobin. In particular, key wavelengths were identified at 540 and 585 nm for PCs 1 and 2, 485 nm for PC 3, and 440 nm for PC 8.

REFERENCES

Chao, K., P. M. Mehl, and Y. R. Chen. 2002a. Use of hyper– and multi–spectral imaging for detection of chicken tumors. *Applied Engineering in Agriculture* 18(1): 113–119.

Chao, K., Y. R. Chen, W. R. Hruschka, and F. B. Gwozdz. 2002b. On–line inspection of poultry carcasses by a dual–camera system. *J. Food Eng.* 51(3): 185–192.

Chen, Y. R., and D. R. Massie. 1993. Visible/near infrared reflectance and interactance spectroscopy for detection of abnormal poultry carcasses. *Transactions of the ASAE* 36(3): 863–889.

Chen, Y. R., B. Park, R. W. Huffman, and M. Nguyen. 1998a. Classification of on–line poultry carcasses with back–propagation neural networks. *J. Food Process Eng.* 21(1): 33–48.

Chen, Y. R., M. Nguyen, and B. Park. 1998b. Neural network with principal component analysis for poultry carcass classification. *J. Food Process Eng.* 21(4): 351–367.

Chen, Y. R., W. R. Hruschka, and H. Early. 2000. A chicken carcass inspection system using visible/near–infrared reflectance: in plant trials. *J. Food Process Eng.* 23(2): 89–99.

Kinsman, D. M., A. W. Kotula, and B. C. Breidenstein. 1994. *Muscle Foods*, 71–74. New York: Chapman and Hall.

Lawrence, K. C., W. R. Windham, B. Park, and R. J. Buhr. 2001. Hyperspectral imaging system for identification of fecal and ingesta contamination on poultry carcasses. ASAE Paper No. 013067. St. Joseph, Mich.: ASAE.

Liu, Y., and Y. R. Chen. 2000. Two–dimensional correlation spectroscopy study of visible and near–infrared spectral variations of chicken meats in cold storage. *Appl. Spectroscopy* 54(10): 1458–1470.

Liu, Y. and Y. R. Chen. 2001. Analysis of visible reflectance spectra of stored, cooked, and diseased chicken meats. *Meat Sci.* 58(4): 395–401.

Liu, Y., Y. R. Chen, and Y. Ozaki. 2000. Two–dimensional visible/near–infrared correlation spectroscopy study of thermal treatment of chicken meats. *J. Agri. Food Chem.* 48(3): 901–908.

Park, B., K. C. Lawrence, W. R. Windham, and R. J. Buhr. 2002. Hyperspectral imaging for detecting fecal and ingesta contamination on poultry carcasses. *Transactions of the ASAE* 45(6): 2017–2026.

Swatland, H. J. 1989. A review of meat spectrophotometry (300 to 800 nm). *Can. Inst. Food Sci. Technol. J.* 22: 390–402.

USDA. 1984. A review of the slaughter regulations under the Poultry Products Inspection Act. Regulations Office, Policy and Program Planning, FSIS, USDA, Washington, D.C.

Windham, W. R., K. C. Lawrence, B. Park, and R. J. Buhr. 2001. Visible/NIR spectroscopy for characterizing fecal contamination of chicken carcasses. ASAE Paper No. 016004. St. Joseph, Mich.: ASAE.